

# Quark Model Calculations of Spectral Functions of Hadronic Current Correlation Functions at Finite Temperature

Hu Li, C. M. Shakin,\* and Qing Sun

*Department of Physics and Center for Nuclear Theory*

*Brooklyn College of the City University of New York*

*Brooklyn, New York 11210*

(Dated: October, 2003)

arXiv:hep-ph/0310254v1 21 Oct 2003

## Abstract

We calculate spectral functions associated with hadronic current correlation functions for vector and pseudoscalar currents at finite temperature. We make use of the Nambu–Jona–Lasinio (NJL) model with temperature-dependent coupling constants and temperature-dependent momentum cutoff parameters. At low energies, good fits are obtained for the spectral functions that were extracted from lattice data by means of the maximum entropy method (MEM). Our model has two parameters which are used to fix the magnitude and position of the large peak seen in the spectral functions. With those two parameters fixed, we obtain a satisfactory fit to the width of the peak. The model then also reproduces the energy of a second peak seen in the spectral functions. In the case of the pseudoscalar spectral function, the calculated peak is about 20 percent higher than that found for the spectral function obtained from the lattice data. However, it appears that the second peak is a lattice artifact [P. Petreczky, private communication] and our fit to the second peak may not be meaningful. We conclude that the NJL model may have a broader range of application than previously considered to be the case, if one allows for significant temperature dependence of the parameters of the model, as well as rather large values of the momentum cutoff parameter. Our treatment of temperature-dependent coupling constants and cutoff parameters is analogous to the procedure introduced by R. Casalbuoni, R. Gatto, G. Nardulli, and M. Ruggieri, [Phys. Rev. D **68**, 034024 (2003)], who make use of the NJL model at finite density and find that they need to use the density-dependent coupling constants and density-dependent cutoff parameters to study matter at high density.

PACS numbers: 12.39.Fe, 12.38.Aw, 14.65.Bt

---

\*email:casbc@cunyvm.cuny.edu

## I. INTRODUCTION

In a member of recent works [1-3] we have calculated various hadronic correlation functions and compared our results to results obtained in lattice simulations of QCD [4-6]. The lattice results for the correlators,  $G(\tau, T)$ , may be used to obtain the corresponding spectral functions,  $\sigma(\omega, T)$ , by making use of the relation

$$G(\tau, T) = \int_0^\infty d\omega \sigma_P(\omega, T) K(\tau, \omega, T), \quad (1.1)$$

where

$$K(\tau, \omega, T) = \frac{\cosh[\omega(\tau - 1/2T)]}{\sinh(\omega/2T)}. \quad (1.2)$$

The procedure to obtain  $\sigma(\omega, T)$  from the knowledge of  $G(\tau, T)$  makes use of the maximum entropy method (MEM) [7-9], since  $G(\tau, T)$  is only known at a limited member of points.

In our previous work we have made use of the Nambu–Jona-Lasinio (NJL) model. The Lagrangian of the generalized NJL model we have used in our studies is

$$\begin{aligned} \mathcal{L} = & \bar{q}(i\gamma - m^0)q + \frac{G_S}{2} \sum_{i=0}^8 [(\bar{q}\lambda^i q)^2 + (\bar{q}i\gamma_5\lambda^i q)^2] \\ & - \frac{G_V}{2} \sum_{i=0}^8 [\bar{q}\lambda^i\gamma_\mu q)^2 + (\bar{q}\lambda^i\gamma_5\gamma_\mu q)^2] \\ & + \frac{G_D}{2} \{\det[\bar{q}(1 + \lambda_5)q] + \det[\bar{q}(1 - \lambda_5)q]\} + \mathcal{L}_{Conf} \end{aligned} \quad (1.3)$$

Here,  $m^0$  is a current quark mass matrix,  $m^0 = \text{diag}(m_u^0, m_d^0, m_s^0)$ . The  $\lambda_i$  are the Gell-Mann (flavor) matrices and  $\lambda^0 = \sqrt{2/3}\mathbf{I}$ , with  $\mathbf{I}$  being the unit matrix. The fourth term is the 't Hooft interaction and  $\mathcal{L}_{Conf}$  represents the model of confinement used in our studies of meson properties. For the present work we neglect the 't Hooft interaction and  $\mathcal{L}_{Conf}$ . Thus, there are essentially three parameters to consider,  $G_S$ ,  $G_V$  and a Gaussian cutoff parameter  $\alpha$ , which restricts the momentum integrals through a factor  $\exp[-\vec{k}^2/\alpha^2]$ . When we use the NJL model to study matter at finite temperature, we introduce the temperature-dependent parameters  $G_S(T)$ ,  $G_V(T)$  and  $\alpha(T)$ . These parameters are adjusted to obtain fits to the spectral functions  $\sigma(\omega, T)$  for  $T/T_c = 1.5$  and  $T/T_c = 3.0$ , which are the values of  $T/T_c$  studied in the lattice simulations of QCD that we consider in this work [10].

TABLE I: Parameters used in the calculation of the results reported in Figs. 1 and 2 are given.

$T/T_c$	0	1.5	3.0
$G_S(\text{ GeV}^{-2})$	13.49 <sup>a</sup>	4.00	1.50
$G_V(\text{ GeV}^{-2})$	11.46 <sup>a</sup>	7.50	2.90 <sup>b</sup>
$\alpha(\text{ GeV}^{-2})$	0.605 <sup>a</sup>	0.850	1.50

a) Values used in Ref. [20],

b) For the calculation reported in Fig. 3, this value is changed to  $G_V = 2.30 \text{ GeV}^{-2}$ .

Our application of a generalized NJL model for the calculation of temperature-dependent hadronic correlation functions has been described in detail in our earlier work [1-3]. For ease of reference, we include the relevant material in the Appendix of this work.

In Section II we present the values obtained in our analysis of the pseudoscalar and vector spectral functions. (The analysis of the axial-vector and scalar spectral functions is quite similar to that given in the Appendix for the vector and pseudoscalar spectral functions.) In Section III we provide some further discussion of our results and some conclusions.

## II. CALCULATION OF HADRONIC CURRENT SPECTRAL FUNCTIONS

In this section we present results obtained for temperature-dependent hadronic current correlation functions making use of the formalism reviewed in the Appendix. Our results may be compared to those presented in Fig. 4 of Ref. [10].

Our calculations are made using the parameters given in Table 1. In Fig. 1 we present values for the pseudoscalar spectral function divided by the square of the energy,  $\sigma/\omega^2$ . The solid line in Fig. 1 is obtained when  $T/T_c = 1.5$  and the dashed line is for  $T/T_c = 3.0$ . In all our calculations we use a Gaussian cutoff,  $\exp[-\vec{k}^2/\alpha^2]$ , when calculating the vacuum polarization functions appearing in the denominator of the spectral function. [ See the Appendix.] The numerator of the spectral function is calculated without a cutoff, so that our result goes over to the perturbative result at large energies. Since the denominator of the spectral function is calculated using our version of NJL model, a cutoff appears naturally in the calculation of the polarization function appearing there.

We note that, once the two parameters of the model ( $G_S$  and  $\alpha$ ) are fixed, the width of the

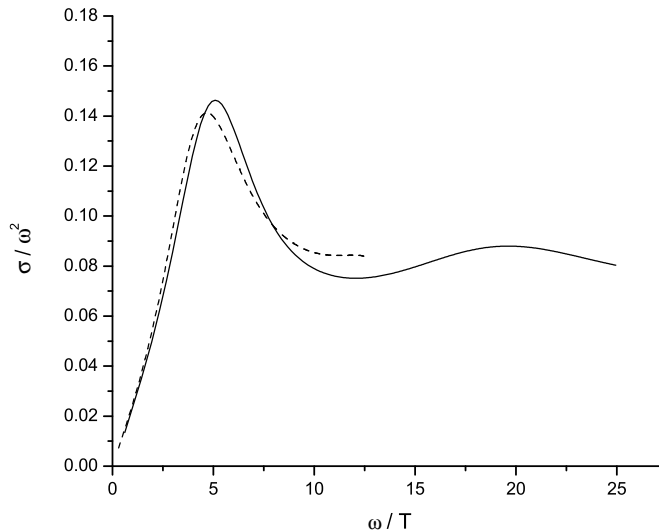


FIG. 1: Calculated values of  $\sigma_P(T)/\omega^2$  are shown as a function of  $\omega/T$  for the model described in the Appendix. [See Table 1.] Comparison may be made to Fig. 4 of Ref. [10] or Fig. 4 of the present work. Here the solid line corresponds to  $T/T_c = 1.5$ , while the dashed line is calculated for  $T/T_c = 3.0$ .

main peak of the pseudoscalar spectral function seen in Fig. 1 is somewhat larger than that seen in Fig. 4. The position of the second broad peak seen in the spectral function obtained in the lattice study at about 3 GeV for  $T/T_c = 1.5$  and at about 6 GeV for  $T/T_c = 3.0$  is satisfactory. For  $T/T_c = 1.5$  the height of the second peak calculated in our work is about 25 percent larger than that seen in Fig. 4 of Ref. [10]. (We recall that the second peaks obtained in the lattice simulations are thought to be unphysical.)

Our results for the vector spectral function is given in Fig. 2, where we have use the parameters of Table 1. In Fig. 4 of Ref. [10] the height of the peak of the vector spectral function for  $T/T_c = 3.0$  is significantly lower than the peak for  $T/T_c = 1.5$ , however, the error is quite large in this case so that our result given in Fig. 2 is still consistent with the lattice data. In Fig. 3, we use a smaller value of  $G_V$  to lower the peak for the  $T/T_c = 3.0$  curve. [See Table 1.] Both the results given in Figs. 2 and 3 are consistent with the values extracted from lattice data for  $T/T_c = 3.0$ , given the large theoretical error in this case.

As noted in the abstract, the second peak seen in the spectral function is thought to be a lattice artifact [11]. Therefore, the fact that we predict the energy of the second peak may

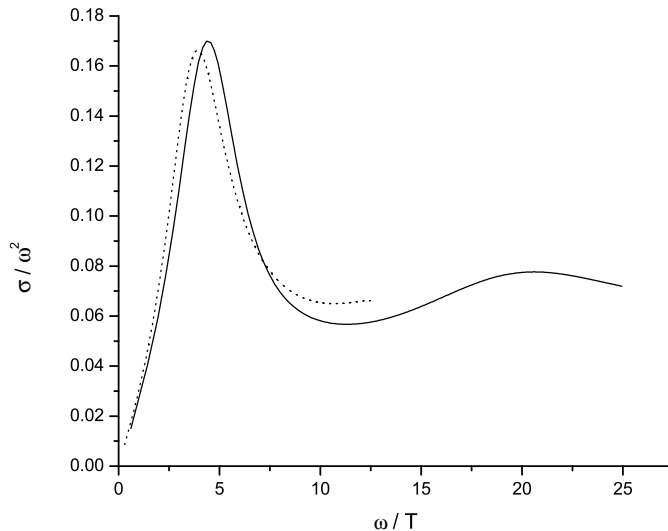


FIG. 2: Calculated values of  $\sigma_V(T)/\omega^2$  are shown as a function of  $\omega/T$ . [See Table 1.] Here the solid line corresponds to  $T/T_c = 1.5$ , while the dotted line is calculated for  $T/T_c = 3.0$ . (See Fig. 4 of Ref. [10] or Fig. 5 of the present work) The theoretical value of  $\sigma_V(T)$  defined in the appendix is here multiplied by  $3/4$  to correspond to the normalization used in the literature [4-6, 10]. [See Eqs. (A30) and (A31)].

not be meaningful.

### III. CONCLUSION

The dynamics of the quark-gluon plasma is a topic of great interest. It has been found that the plasma has a number of features that cannot be described in perturbation theory. The appearance of resonances in the temperature-dependent spectral functions is one of these features. It may be noted in Fig. 5 of Ref. [10] that resonances appear in the scalar, pseudoscalar, vector, and axial-vector spectral functions at about the same energy, which indicates that the state-dependent quark interaction plays a less important role in separating these states in the deconfined phase than in the confined phase. For example, it is well known that the pion loses its character as a Goldstone boson and becomes (approximately) degenerate with the sigma meson in the deconfined phase.

It is of interest to note that the NJL model may be extended to calculate resonances in

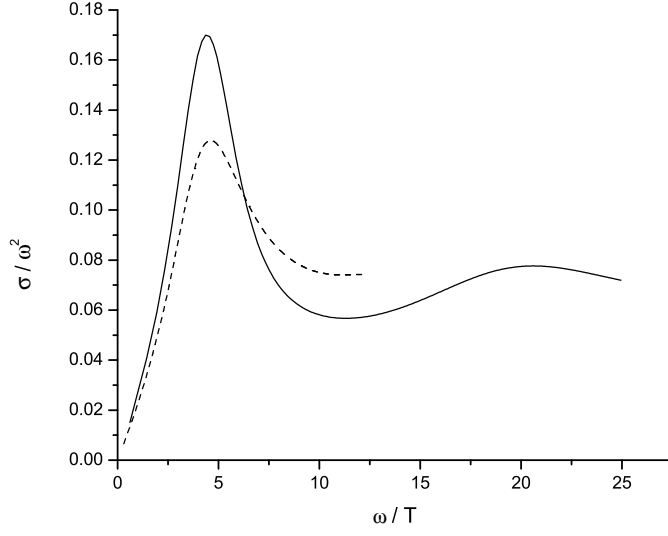


FIG. 3: Calculated values of  $\sigma_V(T)/\omega^2$  are shown. The value of  $G_V$  for the dashed line ( $T/T_c = 3.0$ ) is changed from the value of  $2.9 \text{ GeV}^{-2}$  used for Fig. 2 to  $2.3 \text{ GeV}^{-2}$ . See Fig. 4 of Ref. [10] or Fig. 5 of the present work. Note the large theoretical error for the vector spectral functions in Ref. [10], which makes the height of the first peak somewhat uncertain. (See the comment on the normalization of  $\sigma_V(T)$  given in the caption of Fig. 2.)

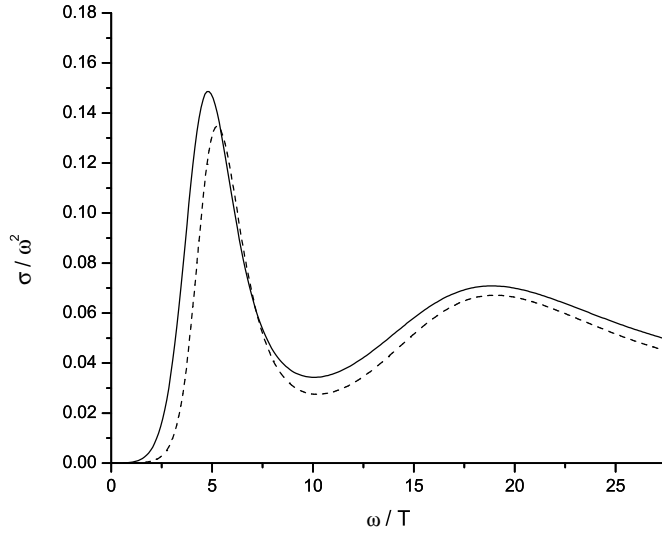


FIG. 4: The spectral function  $\sigma/\omega^2$  for pseudoscalar states obtained by MEM [10] is shown. The solid line is for  $T/T_c = 1.5$  and the dashed line is for  $T/T_c = 3.0$ .

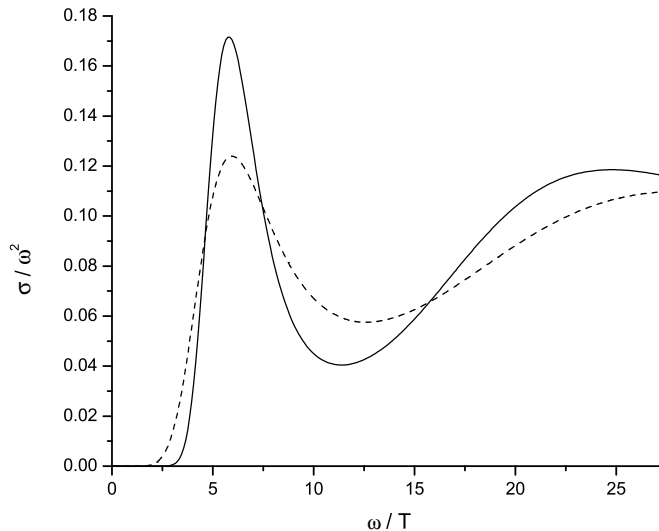


FIG. 5: The spectral function  $\sigma/\omega^2$  for vector states obtained by MEM [10] is shown. See the caption of Fig. 4.

the deconfined phase. In order to describe these resonances we have made the parameters of the model,  $G_S$ ,  $G_V$  and  $\alpha$ , temperature-dependent. We see that our model provides reasonable values for the widths of the resonances and also predicts the position of a second broad resonance seen in the spectral functions. (However, the latter resonance is thought to be a lattice artifact, as noted earlier.)

The temperature-dependent coupling constants and cutoff parameters of our work are analogous to the corresponding density-dependent parameters introduced in Refs. [12] and [13]. Further study of models with temperature-dependent and density-dependent parameters are of interest and a general theoretical formalism for the introduction of such dependencies should be considered.

In future work we also hope to calculate the spatial correlators in the deconfined phase. Some data obtained in lattice studies for such correlation functions are given in Ref. [10].

## APPENDIX

For ease of reference, we present a discussion of our calculation of hadronic current correlators taken from Ref. [3]. The procedure we adopt is based upon the real-time finite-

temperature formalism, in which the imaginary part of the polarization function may be calculated. Then, the real part of the function is obtained using a dispersion relation. The result we need for this work has been already given in the work of Kobes and Semenoff [14]. (In Ref. [14] the quark momentum is  $k$  and the antiquark momentum is  $k - P$ . We will adopt that notation in this section for ease of reference to the results presented in Ref. [14].) With reference to Eq. (5.4) of Ref. [14], we write the imaginary part of the scalar polarization function as

$$\begin{aligned} \text{Im } J_S(P^2, T) = & \frac{1}{2}(2N_c)\beta_S \epsilon(P^0) \int \frac{d^3k}{(2\pi)^3} e^{-\vec{k}^2/\alpha^2} \left( \frac{2\pi}{2E_1(k)2E_2(k)} \right) \\ & \{ (1 - n_1(k) - n_2(k))\delta(P^0 - E_1(k) - E_2(k)) \\ & - (n_1(k) - n_2(k))\delta(P^0 + E_1(k) - E_2(k)) \\ & - (n_2(k) - n_1(k))\delta(P^0 - E_1(k) + E_2(k)) \\ & - (1 - n_1(k) - n_2(k))\delta(P^0 + E_1(k) + E_2(k)) \} . \end{aligned} \quad (\text{A1})$$

Here,  $E_1(k) = [\vec{k}^2 + m_1^2(T)]^{1/2}$ . Relative to Eq. (5.4) of Ref. [14], we have changed the sign, removed a factor of  $g^2$  and have included a statistical factor of  $2N_c$ , where the factor of 2 arises from the flavor trace. In addition, we have included a Gaussian regulator,  $\exp[-\vec{k}^2/\alpha^2]$ . The value  $\alpha = 0.605$  GeV was used in our applications of the NJL model in the calculation of meson properties at  $T = 0$ . We also note that

$$n_1(k) = \frac{1}{e^{\beta E_1(k)} + 1} , \quad (\text{A2})$$

and

$$n_2(k) = \frac{1}{e^{\beta E_2(k)} + 1} . \quad (\text{A3})$$

For the calculation of the imaginary part of the polarization function, we may put  $k^2 = m_1^2(T)$  and  $(k - P)^2 = m_2^2(T)$ , since in that calculation the quark and antiquark are on-mass-shell. In Eq. (A1) the factor  $\beta_S$  arises from a trace involving Dirac matrices, such that

$$\beta_S = -\text{Tr}[(\not{k} + m_1)(\not{k} - \not{P} + m_2)] \quad (\text{A4})$$

$$= 2P^2 - 2(m_1 + m_2)^2 , \quad (\text{A5})$$

where  $m_1$  and  $m_2$  depend upon temperature. In the frame where  $\vec{P} = 0$ , and in the case  $m_1 = m_2$ , we have  $\beta_S = 2P_0^2(1 - 4m^2/P_0^2)$ . For the scalar case, with  $m_1 = m_2$ , we find

$$\text{Im } J_S(P^2, T) = \frac{N_c P_0^2}{4\pi} \left(1 - \frac{4m^2(T)}{P_0^2}\right)^{3/2} e^{-\vec{k}^2/\alpha^2} [1 - 2n_1(k)], \quad (\text{A6})$$

where

$$\vec{k}^2 = \frac{P_0^2}{4} - m^2(T). \quad (\text{A7})$$

For pseudoscalar mesons, we replace  $\beta_S$  by

$$\beta_P = -\text{Tr}[i\gamma_5(\not{k} + m_1)i\gamma_5(\not{k} - \not{P} + m_2)] \quad (\text{A8})$$

$$= 2P^2 - 2(m_1 - m_2)^2, \quad (\text{A9})$$

which for  $m_1 = m_2$  is  $\beta_P = 2P_0^2$  in the frame where  $\vec{P} = 0$ . We find, for the  $\pi$  mesons,

$$\text{Im } J_P(P^2, T) = \frac{N_c P_0^2}{4\pi} \left(1 - \frac{4m^2(T)}{P_0^2}\right)^{1/2} e^{-\vec{k}^2/\alpha^2} [1 - 2n_1(k)], \quad (\text{A10})$$

where  $\vec{k}^2 = P_0^2/4 - m_u^2(T)$ , as above. Thus, we see that the phase space factor has an exponent of 1/2 corresponding to a  $s$ -wave amplitude. For the scalars, the exponent of the phase-space factor is 3/2, as seen in Eq. (A6).

For a study of vector mesons we consider

$$\beta_{\mu\nu}^V = \text{Tr}[\gamma_\mu(\not{k} + m_1)\gamma_\nu(\not{k} - \not{P} + m_2)], \quad (\text{A11})$$

and calculate

$$g^{\mu\nu} \beta_{\mu\nu}^V = 4[P^2 - m_1^2 - m_2^2 + 4m_1 m_2], \quad (\text{A12})$$

which, in the equal-mass case, is equal to  $4P_0^2 + 8m^2(T)$ , when  $m_1 = m_2$  and  $\vec{P} = 0$ . This result will be needed when we calculate the correlator of vector currents. Note that, for the elevated temperatures considered in this work,  $m_u(T) = m_d(T)$  is quite small, so that  $4P_0^2 + 8m_u^2(T)$  can be approximated by  $4P_0^2$ , when we consider the vector current correlation functions. In that case, we have

$$\text{Im } J_V(P^2, T) \simeq \frac{2}{3} \text{Im } J_P(P^2, T). \quad (\text{A13})$$

At this point it is useful to define functions that do not contain that Gaussian regulator:

$$\text{Im } \tilde{J}_P(P^2, T) = \frac{N_c P_0^2}{4\pi} \left(1 - \frac{4m^2(T)}{P_0^2}\right)^{1/2} [1 - 2n_1(k)], \quad (\text{A14})$$

and

$$\text{Im } \tilde{J}_V(P^2, T) = \frac{2}{3} \frac{N_c P_0^2}{4\pi} \left(1 - \frac{4m^2(T)}{P_0^2}\right)^{1/2} [1 - 2n_1(k)], \quad (\text{A15})$$

For the functions defined in Eq. (A14) and (A15) we need to use a twice-subtracted dispersion relation to obtain  $\text{Re } \tilde{J}_P(P^2, T)$ , or  $\text{Re } \tilde{J}_V(P^2, T)$ . For example,

$$\begin{aligned} \text{Re } \tilde{J}_P(P^2, T) = \text{Re } \tilde{J}_P(0, T) + \frac{P^2}{P_0^2} [\text{Re } \tilde{J}_P(P_0^2, T) - \text{Re } \tilde{J}_P(0, T)] \\ + \frac{P^2(P^2 - P_0^2)}{\pi} \int_{4m^2(T)}^{\tilde{\Lambda}^2} ds \frac{\text{Im } \tilde{J}_P(s, T)}{s(P^2 - s)(P_0^2 - s)}, \end{aligned} \quad (\text{A16})$$

where  $\tilde{\Lambda}^2$  can be quite large, since the integral over the imaginary part of the polarization function is now convergent. We may introduce  $\tilde{J}_P(P^2, T)$  and  $\tilde{J}_V(P^2, T)$  as complex functions, since we now have both the real and imaginary parts of these functions. We note that the construction of either  $\text{Re } J_P(P^2, T)$ , or  $\text{Re } J_V(P^2, T)$ , by means of a dispersion relation does not require a subtraction. We use these functions to define the complex functions  $J_P(P^2, T)$  and  $J_V(P^2, T)$ .

In order to make use of Eq. (A16), we need to specify  $\tilde{J}_P(0)$  and  $\tilde{J}_P(P_0^2)$ . We found it useful to take  $P_0^2 = -1.0 \text{ GeV}^2$  and to put  $\tilde{J}_P(0) = J_P(0)$  and  $\tilde{J}_P(P_0^2) = J_P(P_0^2)$ . The quantities  $\tilde{J}_V(0)$  and  $\tilde{J}_V(P_0^2)$  are determined in an analogous function. This procedure in which we fix the behavior of a function such as  $\text{Re } \tilde{J}_V(P^2)$  or  $\text{Re } \tilde{J}_V(P^2)$  is quite analogous to the procedure used in Ref. [15]. In that work we made use of dispersion relations to construct a continuous vector-isovector current correlation function which had the correct perturbative behavior for large  $P^2 \rightarrow -\infty$  and also described the low-energy resonance present in the correlator due to the excitation of the  $\rho$  meson. In Ref. [15] the NJL model was shown to provide a quite satisfactory description of the low-energy resonant behavior of the vector-isovector correlation function.

We now consider the calculation of temperature-dependent hadronic current correlation functions. The general form of the correlator is a transform of a time-ordered product of currents,

$$iC(P^2, T) = \int d^4x e^{iP \cdot x} \ll T(j(x)j(0)) \gg, \quad (\text{A17})$$

where the double bracket is a reminder that we are considering the finite temperature case.

For the study of pseudoscalar states, we may consider currents of the form  $j_{P,i}(x) = \tilde{q}(x)i\gamma_5\lambda^i q(x)$ , where, in the case of the  $\pi$  mesons,  $i = 1, 2$  and  $3$ . For the study of scalar-isoscalar mesons, we introduce  $j_{S,i}(x) = \tilde{q}(x)\lambda^i q(x)$ , where  $i = 0$  for the flavor-singlet current and  $i = 8$  for the flavor-octet current [16].

In the case of the pseudoscalar-isovector mesons, the correlator may be expressed in terms of the basic vacuum polarization function of the NJL model,  $J_P(P^2, T)$  [17-19]. Thus,

$$C_P(P^2, T) = J_P(P^2, T) \frac{1}{1 - G_P(T)J_P(P^2, T)}, \quad (\text{A18})$$

where  $G_P(T)$  is the coupling constant appropriate for our study of  $\pi$  mesons. We have found  $G_P(T) = 13.49 \text{ GeV}^{-2}$  by fitting the pion mass in a calculation made at  $T = 0$ , with  $m_u = m_d = 0.364 \text{ GeV}$ . The result given in Eq. (A18) is only expected to be useful for small  $P^2$ , since the Gaussian regulator strongly modifies the large  $P^2$  behavior. Therefore, we suggest that the following form is useful, if we are to consider the larger values of  $P^2$ .

$$\frac{C_P(P^2, T)}{P^2} = \left[ \frac{\tilde{J}_P(P^2, T)}{P^2} \right] \frac{1}{1 - G_P(T)J_P(P^2, T)}. \quad (\text{A19})$$

(As usual, we put  $\vec{P} = 0$ .) This form has two important features. At large  $P_0^2$ ,  $\text{Im} C_P(P_0, T)/P_0^2$  is a constant, since  $\text{Im} \tilde{J}_P(P_0^2, T)$  is proportional to  $P_0^2$ . Further, the denominator of Eq. (A19) goes to 1 for large  $P_0^2$ . On the other hand, at small  $P_0^2$ , the denominator is capable of describing resonant enhancement of the correlation function. As we have seen, the results obtained when Eq. (A19) is used appear quite satisfactory. (We may again refer to Ref. [15], in which a similar approximation is described.)

For a study of the vector-isovector correlators, we introduce conserved vector currents  $j_{\mu,i}(x) = \tilde{q}(x)\gamma_\mu\lambda_i q(x)$  with  $i=1, 2$  and  $3$ . In this case we define

$$J_V^{\mu\nu}(P^2, T) = \left( g^{\mu\nu} - \frac{P^\mu P^\nu}{P^2} \right) J_V(P^2, T) \quad (\text{A20})$$

and

$$C_V^{\mu\nu}(P^2, T) = \left( g^{\mu\nu} - \frac{P^\mu P^\nu}{P^2} \right) C_V(P^2, T), \quad (\text{A21})$$

taking into account the fact that the current  $j_{\mu,i}(x)$  is conserved. We may then use the fact that

$$J_V(P^2, T) = \frac{1}{3} g_{\mu\nu} J_V^{\mu\nu}(P^2, T) \quad (\text{A22})$$

and

$$\text{Im } J_V(P^2, T) = \frac{2}{3} \left[ \frac{P_0^2 + 2m_u^2(T)}{4\pi} \right] \left( 1 - \frac{4m_u^2(T)}{P_0^2} \right)^{1/2} e^{-\vec{k}^2/\alpha^2} [1 - 2n_1(k)] \quad (\text{A23})$$

$$\simeq \frac{2}{3} \text{Im } J_P(P^2, T). \quad (\text{A24})$$

(See Eq. (A7) for the specification of  $k = |\vec{k}|$ .) We then have

$$C_V(P^2, T) = \tilde{J}_V(P^2, T) \frac{1}{1 - G_V(T) J_V(P^2, T)}, \quad (\text{A25})$$

where we have introduced

$$\text{Im } \tilde{J}_V(P^2, T) = \frac{2}{3} \left[ \frac{P_0^2 + 2m_u^2(T)}{4\pi} \right] \left( 1 - \frac{4m_u^2(T)}{P_0^2} \right)^{1/2} [1 - 2n_1(k)] \quad (\text{A26})$$

$$\simeq \frac{2}{3} \text{Im } \tilde{J}_P(P^2, T). \quad (\text{A27})$$

In the literature,  $\omega$  is used instead of  $P_0$  [4-6]. We may define the spectral functions

$$\sigma_V(\omega, T) = \frac{1}{\pi} \text{Im } C_V(\omega, T), \quad (\text{A28})$$

and

$$\sigma_P(\omega, T) = \frac{1}{\pi} \text{Im } C_P(\omega, T), \quad (\text{A29})$$

Since different conventions are used in the literature [4-6], we may use the notation  $\bar{\sigma}_P(\omega, T)$  and  $\bar{\sigma}_V(\omega, T)$  for the spectral functions given there. We have the following relations:

$$\bar{\sigma}_P(\omega, T) = \sigma_P(\omega, T), \quad (\text{A30})$$

and

$$\frac{\bar{\sigma}_V(\omega, T)}{2} = \frac{3}{4} \sigma_V(\omega, T), \quad (\text{A31})$$

where the factor 3/4 arises because, in Refs. [4-6], there is a division by 4, while we have divided by 3, as in Eq. (A22).

---

[1] Bing He, Hu Li, C. M. Shakin, and Qing Sun, Phys. Rev. D **67**, 014022 (2003).

- [2] Bing He, Hu Li, C. M. Shakin, and Qing Sun, Phys. Rev. D **67**, 114012 (2003).
- [3] Bing He, Hu Li, C. M. Shakin, and Qing Sun, Phys. Rev. C **67**, 065203 (2003).
- [4] I. Wetzorke, F. Karsch, E. Laermann, P. Petreczky, and S. Stickan, Nucl. Phys. B (Proc. Suppl.) **106**, 510 (2002)
- [5] F. Karsch, S. Datta, E. Laermann, P. Petreczky, and S. Stickan, and I. Wetzorke, Nucl. Phys. A **715**, 701c (2003)
- [6] F. Karsch, E. Laermann, P. Petreczky, S. Stickan, and I. Wetzorke, Phys. Lett. B **530**, 147 (2002).
- [7] M. Asakawa, T. Hatsuda and Y. Nakahara, Nucl. Phys. A **715**, 863 (2003)
- [8] T. Umeda, K. Nomura and H. Matsufuru, hep-ph/0211003.
- [9] I. Wetzorke, hep-ph/0305012. (Invited talk at the 'Seventh Workshop on Quantum Chromodynamics', Villefranche-sur-mer, France, Jan. 6-10, 2003)
- [10] P. Petreczky, hep-ph/0305189.
- [11] P. Petreczky, private communication.
- [12] M. Ruggieri, hep-ph/0310145.
- [13] R. Casalbuoni, R. Gatto, G. Nardulli, and M. Ruggieri, Phys. Rev. D **68**, 034024 (2003).
- [14] R. L. Kobes and G. W. Semenoff, Nucl. Phys. B **260**, 714 (1985).
- [15] C. M. Shakin, Wei-Dong Sun, and J. Szweda, Ann. of Phys. (NY) **241**, 37 (1995).
- [16] Hu Li and C. M. Shakin, hep-ph/0209136.
- [17] S. P. Klevansky, Rev. Mod. Phys. **64**, 649 (1992).
- [18] T. Hatsuda and T. Kunihiro, Phys. Rep. **247**, 221 (1994).
- [19] U. Vogl and W. Weise, Prog. Part. Nucl. Phys. **27**, 195 (1991).
- [20] Hu Li and C. M. Shakin, Phys. Rev. D **66**, 074016 (2002).